Universality of chaotic rare fluctuations in a locally coupled phase map model

Takeshi Watanabe,[1,*] Yasuhiro Tsubo,[2,†] and Hirokazu Fujisaka[3,‡]
[1]*Division of Global Development Science, Graduate School of Science and Technology, Kobe University, Kobe 657-8501, Japan*
[2]*Department of Physics, Graduate School of Sciences, Kyoto University, Kyoto 606-8502, Japan*
[3]*Department of Applied Analysis and Complex Dynamical Systems, Graduate School of Informatics, Kyoto University, Kyoto 606-8501, Japan*
(Received 6 July 2001; published 24 January 2002)

Chaotic fluctuations of the order parameter in a coupled two-dimensional phase map model are numerically investigated. We discuss the system-size N dependence of the statistical properties of *rare fluctuations* observed in the transition range between the quasiordered chaotic state and the fully developed one. It is found that the normalized probability distribution function (PDF) has a unique functional form irrespective of N. The asymptotic form of the PDF is discussed in connection with the universal distribution for correlated systems proposed by Bramwell *et al.* [Nature (London) **396**, 552 (1998)]. Moreover, it is observed that the power spectrum $P_N(\omega)$ of rare fluctuations asymptotically takes the power-law form $P_N(\omega)\sim\omega^{-(1+\alpha)}$ ($\alpha=0.6\sim0.7$) irrespective of N. This result suggests that the temporal correlation decays as a stretched exponential.

DOI: 10.1103/PhysRevE.65.026213 PACS number(s): 05.45.−a, 05.10.−a, 95.10.Fh

I. INTRODUCTION

Strong correlations of fluctuations over a wide range of times and spaces are typical of nonlinear and nonequilibrium phenomena. In fluid mechanics, for example, the velocity fluctuations observed in fully developed turbulence show strong and self-similar correlations from the energy injection scale L to the dissipation scale η. Universal statistics in the intermediate scale (the so-called inertial subrange) have been explored by many researchers [1]. Similar correlated fluctuations are also observed in critical phenomena. Magnetic fluctuations of spin systems at the critical temperature indicate the long-range magnetic order over scales ranging from the lattice constant to the system size. It is well known that critical exponents characterizing the statistical nature of critical phenomena are universal in the sense that they are independent of microscopic physical details [2].

Consider the fluctuations of coarse-grained physical quantities over a scale l that satisfies the condition $l_{min}\ll l \ll l_{max}$, where l_{max} (l_{min}) is a well-defined effective largest (smallest) scale in the system. In the aforementioned physical systems, fluctuations on a scale l indicate strong correlations, represented by a power-law decay with respect to l. Fluctuation on this scale are characterized from the viewpoint of ''statistical self-similarity'' of fluctuations, irrespective of the details of the physical systems under consideration [3]. In treating a physical quantity defined at l_{max}, e.g., the averaged energy dissipation rate in turbulence, we regard it as constant because the dispersion of fluctuations at l_{max} is much smaller than that at l. However, the self-similar fluctuations reach the scale l_{max} when the correlation length is larger than l_{max}. In this case, we cannot neglect the fluctuations at l_{max} because they are connected to those at smaller scales through the strong correlations of fluctuations. In addition, the cutoff of the self-similar nature at scale l_{max} is affected by the boundary conditions. Therefore, it seems that the statistical nature at l_{max} depends on the system because a quantity coarse-grained at the largest scale, denoted as a ''global measure'' in this paper, is affected by the details of the boundary conditions. In a recent study by Bramwell, Holdsworth, and Pinton (BHP) [4], however, it is suggested that global measure fluctuations defined in both turbulence and critical phenomena indicate universal statistical features. Their arguments are briefly reviewed as follows.

In experimental von-Karman turbulent flow, on the one hand, the global measure defined by the power consumption fluctuations of a turbulent flow maintained at constant Reynolds number (Re) shows a unique functional form for the normalized probability distribution function (PDF), irrespective of Re [5,6]. In a finite two-dimensional (2D) harmonic XY model (2DHXY), on the other hand, fluctuations of the global measure, i.e., the magnetic scalar order parameter, are investigated in [7,8]. A unique form of the PDF, irrespective of the number of degrees of freedom (system size) N, was found by Monte Carlo simulation. Furthermore, BHP [4] pointed out that both PDF forms of global measures obtained in turbulence and critical phenomena overlap quite well in an extended range. They discussed this universal nature of global fluctuations from the viewpoint of strong correlations, self-similarity, and system size effects. The global measures defined in these systems are spatially coarse-grained variables. If the spatial correlation length of the fluctuations is extremely small in comparison with the system size, we can expect that the PDF's of global measures should be Gaussian by the central limit theorem. However, the observed PDF show the following specific characteristics: (1) the PDF's are strongly asymmetrical and non-Gaussian since the strong spatial correlations affect the statistical properties of the global measures, and (2) the normalized PDF's overlap on a single curve. Furthermore, this universal PDF is observed for global measures defined in several strongly correlated physical systems [9].

Strong correlations and fluctuations obeying non-Gaussian PDF's are also observed in the statistics of chaotic dynamical systems. Several spatially extended dynamical

*Electronic address: watanabe@shizen.sci.kobe-u.ac.jp
†Electronic address: tsubo@ton.scphys.kyoto-u.ac.jp
‡Electronic address: fujisaka@i.kyoto-u.ac.jp

systems such as reaction diffusion systems that display chemical oscillations or collective motion in interacting limit cycle oscillators are proposed as models for investigating nonlinear and nonequibilium dynamics. One of the important and basic models is a complex time-dependent Ginzburg-Landau (CTDGL) equation, which describes the spatiotemporal dynamics near a Hopf bifurcation point [10]. Based on this model equation, statistical features of several spatiotemporal chaotic states in chemical turbulence have been investigated both theoretically and numerically [11].

In this paper, we focus on the spatiotemporal dynamics of a coupled phase map system that approximately describes the long-time behavior of the spatially coupled CTDGL equation. Especially, we investigate the statistical properties of order-parameter fluctuations in the phase map model in the weak-coupling limit, where the dynamical variables and the order parameter are corresponding to the orientation of each spin and the mean scalar magnetic intensity, respectively.

The main difference between the chaotic phase map and XY spin systems is the origin of the fluctuations; in the former case, they are caused by chaos intrinsic to the system, while in the latter, they are caused by thermal noise. Thus, the fluctuations in the chaotic phase map originate from strong nonlinearity intrinsic to the system. We discuss the parameter dependences of several statistical quantities describing the order-parameter fluctuations. Strongly non-Gaussian PDF's are observed in the specific spatiotemporal chaotic state. Especially, the system-size dependence of these PDF's are investigated in detail in connection with the universal PDF for turbulence and critical phenomena proposed by BHP [4,9]. Moreover, we refer to the statistical properties of rare dynamical fluctuations by investigating the power spectrum when the PDF shows the universal form proposed by BHP.

This paper is organized as follows. Section II introduces the phase map model. In Sec. III, the global features of the spatiotemporal dynamics are investigated for several values of the system parameters. In Sec. IV, we discuss the universal nature of the PDF for the order-parameter fluctuations in the specific spatiotemporal chaotic state. In Sec. V, the PDF obtained in the phase map model is compared with the analytic form proposed by BHP [9] and a stochastic phase map model phenomenologically constructed on the basis of the chaotic phase map. In Sec. VI, the temporal correlations of rare fluctuations are studied by observing the asymptotic form of the power spectrum and its system-size dependence. In Sec. VII, we summarize the results obtained in this paper.

II. TWO-DIMENSIONAL COUPLED PHASE MAP SYSTEMS

It is difficult to investigate the long-time behavior of spatially extended or coupled CTDGL equations because of the large number of degrees of freedom. Numerical integration is also restricted by the current limits of computational power. A possible approach in this situation is to construct a dynamical model to investigate the long-time behavior of coupled CTDGL equations. We can discuss dynamical or statistical properties of spatio-temporal dynamics based on this model theoretically and numerically. Such a model for this purpose, the coupled Ginzburg-Landau Map (CGLM), was proposed by Uchiyama and Fujisaka [12]. The CGLM, which is composed of effective phase variables, approximately describes the long-time behavior of the coupled CTDGL, where the amplitude included in the CTDGL is eliminated in the long-time limit. This model is represented as

$$e^{i\theta_{t+1}^{(\mathbf{r})}} = h_t^{(\mathbf{r})} \left| h_t^{(\mathbf{r})} \right|^{-(1+iC)}, \quad h_t^{(\mathbf{r})} = \sum_{\mathbf{r}'} J_{\mathbf{r}\mathbf{r}'} e^{i\theta_t^{(\mathbf{r}')}}, \tag{1}$$

where $\theta_t^{(\mathbf{r})}$ denotes the phase variable describing the state of the oscillator at the discrete grid point $\mathbf{r}=\{x,y,\ldots,\}$ $(=0,1,2,\ldots,)$ and time step $t(=0,1,2,\ldots,)$. The $J_{\mathbf{r}\mathbf{r}'}$ represents the complex coupling matrix determining the interactions among the oscillators. If $\Sigma_{\mathbf{r}'} J_{\mathbf{r}\mathbf{r}'}$ is independent of $\mathbf{r}$, Eq. (1) has the spatially synchronized particular solution $\theta_t^{(\mathbf{r})} = \theta_t^s$ as

$$\theta_{t+1}^s = \theta_t^s + \xi - C \ln |w|, \tag{2}$$

where $w = \Sigma_{\mathbf{r}'} J_{\mathbf{r}\mathbf{r}'} = |w| e^{i\xi}$ is independent of $\mathbf{r}$. We may apply several complex coupling matrices for modeling particular physical systems. Globally and randomly coupled cases were investigated in detail in [12]. The parameter C is real and is a characteristic parameter of this model. Equation (1) for $C=0$ is equivalent to the Noest model, which is well known as a model for neural networks [13]. A study applying this model with $C \neq 0$ to a neural network was carried out in Ref. [14].

In this paper, we propose a local coupling among the oscillators, so that such oscillator interacts with its nearest neighbors. The coupling matrix is given by

$$J_{\mathbf{r}\mathbf{r}'} = \begin{cases} 1 & (|\mathbf{r}-\mathbf{r}'|=0) \\ \kappa e^{i\beta} & (|\mathbf{r}-\mathbf{r}'|=1) \\ 0 & (\text{otherwise}), \end{cases} \tag{3}$$

where κ and β are real. This is the fundamental model for investigating the long-time dynamics of the collective motion of locally interacting oscillators. Here, we use a two-dimensional (2D) square lattice, $\mathbf{r}=(x,y)(\{x,y\} = 1,2,\ldots,n)$ with periodic boundary conditions. This 2D phase model has a spatially synchronized particular solution since the coupling matrix (3) in 2D satisfies the equation

$$w = \sum_{\mathbf{r}'} J_{\mathbf{r}\mathbf{r}'} = 1 + 4\kappa e^{i\beta}, \tag{4}$$

independent of $\mathbf{r}$. The temporal evolution of the particular solution is obtained by substituting Eq. (4) into Eq. (2).

We define the order-parameter M_t to characterize the global state of the phase map system by

$$Z_t = \frac{1}{N} \sum_{\{x,y\}=1}^{N} e^{i\theta_t^{(x,y)}} = X_t + iY_t, \tag{5}$$

$$M_t = |Z_t| = \sqrt{X_t^2 + Y_t^2}, \tag{6}$$

where the summation is taken over all $N = n \times n$ spatial points. The order-parameter M_t represents the degree of synchronization of the oscillators. It is unity if all oscillators are spatially synchronized, while it is close to zero when they fluctuate randomly. This quantity corresponds to the instantaneous scalar magnetic intensity in an XY spin system. In a chaotic state, the global measure M_t fluctuates within $[0,1]$. The macroscopic behavior of the phase dynamics is characterized by the fluctuations of M_t and their statistical properties, and M_t is the global measure of the phase map system.

The locally coupled CGLM contains three control parameters, C, κ, and β. Various dynamic aspects are observed by choosing appropriate parameter values [15]. The most important parameter is C, which controls the complexity of the dynamics. In the κ-β parameter region where the unstable uniform oscillation and the inverse-phase state coexist, the system attains several spatiotemporal chaotic states as C is gradually increased from zero. Spatial structure is observed for $C \sim 1$. A developed spatiotemporal chaotic state is established in the large $C(\gg 1)$ region, where the system behavior is fully complex both spatially and temporally. Observing the dynamic features of M_t, we may, on the whole, divide the states of motion into three groups, (i) coherent states ($C < 1$), (ii) weakly spatio-temporal chaotic states ($C \sim 1$), and (iii) turbulent states ($C \gg 1$). The system falls onto a particular solution in the coherent state, where fluctuations in M_t are not observed. M_t equals unity because all the oscillators are perfectly synchronized. Fluctuations in M_t are observed in the second region, where the system shows weak chaotic behavior with a spatially coherent structure. In the turbulent state, strongly developed spatiotemporal chaos is observed, and M_t fluctuates near zero.

When we consider the weak coupling limit of the coupled CGLM, i.e., $\kappa \ll 1$, the equation may be approximated as

$$\theta_{t+1}^{(x,y)} = \theta_t^{(x,y)} + D \sum_{n.n.} \sin(\theta_t^{(x',y')} - \theta_t^{(x,y)} + \phi), \tag{7}$$

$$D = \kappa\sqrt{1+C^2}, \quad \phi = \beta - \tan^{-1} C, \tag{8}$$

to $O(\kappa)$, where $\Sigma_{n.n.}$ indicates summation over the nearest neighbors of the site (x,y). Note that the control parameters in the coupled CGLM are effectively reduced to two parameters (D,ϕ) in Eq. (7). The spatially synchronized solution for this model satisfies $\theta_{t+1}^s = \theta_t^s + 4D\sin(\phi)$. This particular solution is also obtained from Eqs. (2) and (4) in the $\kappa \to 0$ limit. Equation (7) with $\phi = 0$,

$$\theta_{t+1}^{(x,y)} = \theta_t^{(x,y)} + D \sum_{n.n.} \sin(\theta_t^{(x',y')} - \theta_t^{(x,y)}) \tag{9}$$

has the specific characteristic that the spatially synchronized solution is temporally constant $\theta_t^s = \theta_0$.

Next, we consider the linear stability of the synchronized oscillation of Eq. (9) by putting $\delta_t^{(x,y)} = \theta_t^{(x,y)} - \theta_0$. The stability condition for $\delta_t^{(x,y)} = \delta_t^0 e^{i(q_x x + q_y y)}$ is given by $-1 < 1 - 4D[\sin^2(q_x/2) + \sin^2(q_y/2)] < 1$. Therefore, the synchronized solution is linearly stable for

$$0 < D < \frac{1}{4}. \tag{10}$$

The synchronized solution becomes unstable for $D > 1/4$, where the nonlinearity plays an important role for the dynamics. Numerical simulation shows that a chaotic motion appears in this region. The parameters included in Eq. (9) are the coupling-constant D and the number of oscillators (system size) N. Depending on D, several states are observed. In the large $D(\gg 1)$ region, especially, we expect that fully developed spatial and temporal chaotic states are observed because the inequality $D \gg 1$ means that $C \gg 1$ holds in CGLM. Another important aspect is that Eq. (9) has a conserved quantity under periodic boundary conditions. In fact, one may easily prove that the quantity

$$\theta_c = \sum_{\{x,y\}=1}^{N} \theta_t^{(x,y)} \tag{11}$$

is a constant of the motion. Thus, the system Eq. (9) has $N - 1$ degrees of freedom.

A coupled phase map model such as Eq. (9) has been investigated for the globally coupled case [16]. To the best of our knowledge, there have been no previous studies of the locally coupled case. We numerically investigate the collective chaotic motion and statistical properties of the M_t fluctuations in Eq. (9). Hereafter, this model will be called the locally coupled sine-circle map (LCSCM).

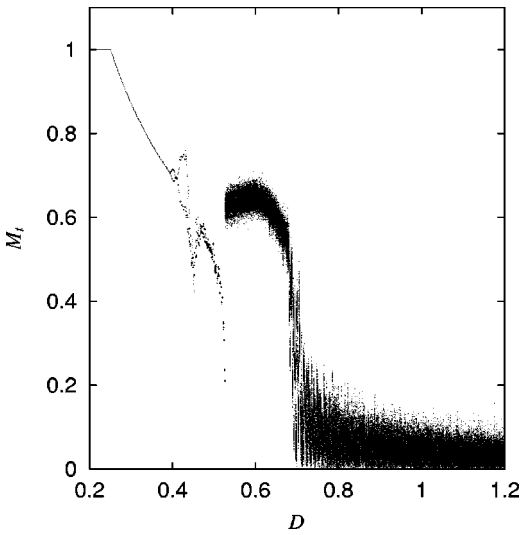

FIG. 1. Bifurcation diagram of the order-parameter M_t in the LCSCM, shown vs D. The system size is fixed at $N = 32^2$.

III. GLOBAL FEATURES OF THE LOCALLY COUPLED SINE-CIRCLE MAP

In order to obtain the global dynamical features of the LCSCM, we investigate how the fluctuations in M_t depend on the parameter D for fixed N. Figure 1 shows the bifurca-

tion diagram of M_t with $N=32^2$, based on 128 data points for each value of D. For each data point, the system was started at $\theta_0^{(x,y)}=0.01\pi r^{(x,y)}$, $r^{(x,y)}$ being independent uniform random numbers about each sites with width $[-1,1]$, and 65 536 time steps were discarded to allow transients to decay. From the results shown in Fig. 1, the dynamics of M_t is roughly characterized as follows. In the $0<D<1/4$ region, M_t equals unity because the spatially synchronized state is stable in this parameter region. The spatially uniform state becomes unstable for $D>1/4$. Until $D\simeq 0.4$, M_t falls on the fixed-point solutions below unity. The dynamics of M_t for $0.4<D<0.55$ indicates periodic motion. In this region, however, the relaxation time for the steady state is quite long, and in addition, these periodic solutions sensitively depend on the initial conditions. The state of motion drastically changes around $D\simeq 0.55$, and M_t shows chaotic fluctuations for $D>0.55$. As D increases further, we notice that the state of motion changes around $D\simeq 0.7$ from $M_t\simeq 0.65$ to $M_t\simeq 0$. This result implies that as D is increased, a transition between a spatially coherent quasiordered chaotic state and a fully developed spatiotemporal chaotic one occurs.

Next, in order to characterize the chaotic behaviors of M_t, we investigate how statistical quantities change as the parameters are changed. The average value $a_N=\langle M_t\rangle$ and the standard deviation $\sigma_N=\langle(M_t-\langle M_t\rangle)^2\rangle^{1/2}$ are analyzed for several values of D and N. Here, $\langle\cdots\rangle$ means the long-time average. Figure 2 shows the D and N dependences of (a) a_N and (b) $\sqrt{N}\sigma_N$, where D is varied between $0.55-1.05$ with increments of 5×10^{-3} for $N=16^2$, 32^2, 48^2, and 64^2. The average for each run was taken over 327 680 time steps after eliminating the transient 20 000 steps. In the $0.55<D<0.65$ range, $a_N\simeq 0.65$, but it decreases rapidly around $0.65<D<0.7$. This result clearly indicates that there is a transition between a spatially coherent quasiordered chaotic state and a fully developed chaotic one in the range $0.65<D<0.7$. This nature is also qualitatively independent of the system size N. Indications of a transition is also observed for $\sqrt{N}\sigma_N$ in the $0.65<D<0.7$ region, where the fluctuation around a_N rapidly increases. On the other hand, the other region is not almost independent of system size N. This means that the standard deviation decreases as $\sigma_N\sim N^{-1/2}$, so that, as discussed in the next section, the spatial correlation lengths of fluctuations are extremely small in these parameter values. The position of the sharp peak in the transition region of $\sqrt{N}\sigma_N$ appears to converge to an N-independent value near $D\simeq 0.68$ as N increases. The large fluctuations in M_t in this parameter range suggests a specific transition among spatiotemporal chaotic states. The incipient divergence of $\sqrt{N}\sigma_N$ reminds us of the interrelation between the present chaotic phase system and the 2DHXY system when we regard the parameter D and σ_N as analogous to the temperature and susceptibility, respectively.

Moreover, we investigate the behavior of normalized moments. The coefficient of variation $CV_N\equiv\sigma_N/a_N$ and the skewness coefficient $S_N\equiv\langle(M_t-\langle M_t\rangle)^3\rangle/\sigma_N^3$ for several values of N are shown in Figs. 3(a) and 3(b), respectively. The numerical conditions for Fig. 3 are the same as for Fig. 2. We can recognize that CV_N and S_N sensitively depend on

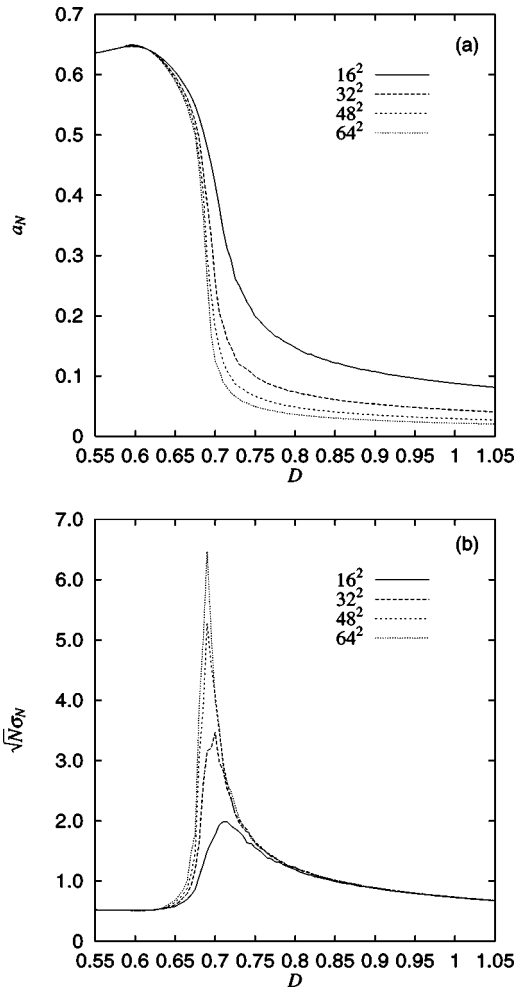

FIG. 2. The D dependences of (a) the average a_N and (b) the standard deviation σ_N of M_t in the LCSCM. Each line represents a different system size, $N=16^2$, 32^2, 48^2, and 64^2.

D in the transition range represented in Figs. 2(a) and 2(b). In this range, however, one should notice that a crossing point of the each lines in Fig. 3(a) is observed near $D=0.68$, and it is close to the minimum positions of Fig. 3(b), which seems to be independent of N. These facts may be possible to determine a transition point for the infinite system size in detail. The studies for this purpose will be reported in the future paper.

Another characteristic behavior is observed in the large D region ($D>0.7$), where CV_N and S_N are asymptotically constant irrespective of D and N. This result is explained as follows. When D is sufficiently large, M_t fluctuates near zero because the motion of the oscillators attains a fully developed chaotic state, and they thus evolve almost randomly. This implies that X_t and Y_t are regarded as averages of N-independent random variables. The probability distribution functions (PDF) of X_t and Y_t are evaluated as normal distributions (Gaussians) for $N\gg 1$ (the central limit theorem). Moreover, we can expect that $\langle X_t\rangle\simeq 0$, $\langle Y_t\rangle\simeq 0$, and $\langle X_tY_t\rangle\simeq\langle X_t\rangle\langle Y_t\rangle\simeq 0$ are approximately satisfied for $D\gg 1$. This is verified if $\theta_t^{(x,y)}$ are represented by independent uniform random numbers with large dispersion. Consequently, it

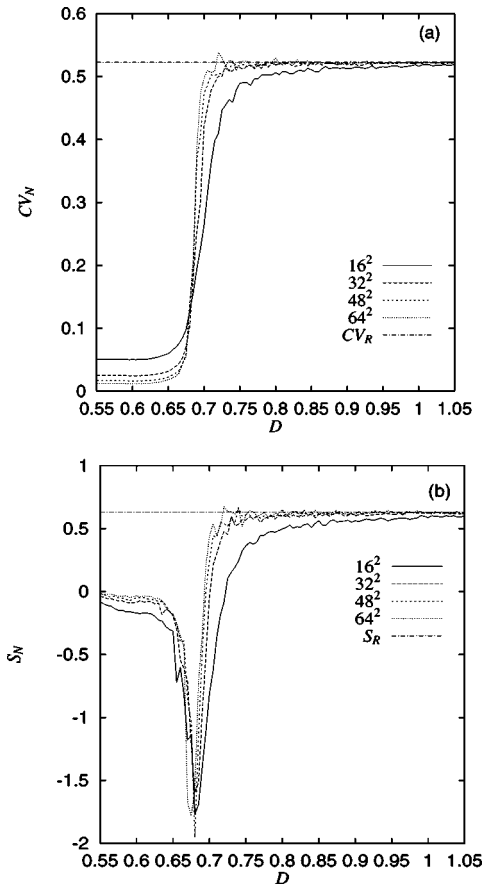

FIG. 3. The D dependences of the normalized moments, (a) the coefficient of variation CV_N, and (b) the skewness coefficient S_N. CV_R and S_R are evaluated by the Rayleigh distribution. For details, see the text.

is expected that X_t and Y_t obey identical and independent normal distributions, so that the PDF of $M_t = \sqrt{X_t^2 + Y_t^2}$, $P_N(M) = \langle \delta(M - M_t) \rangle$, is the Rayleigh distribution

$$P_N(M) = \frac{\pi M}{2a_N^2} \exp\left(- \frac{\pi M^2}{4a_N^2} \right). \tag{12}$$

The corresponding normalized moments, CV_R and S_R are obtained as

$$CV_R = \left(\frac{4-\pi}{\pi} \right)^{1/2} \simeq 0.52, \tag{13}$$

$$S_R = \frac{2(\pi - 3)\pi^{1/2}}{(4-\pi)^{3/2}} \simeq 0.63. \tag{14}$$

Figure 3 clearly shows that CV_N and S_N asymptotically approach to CV_R and S_R, irrespective of N. In the $0.55 < D < 0.65$ region, on the other hand, S_N is near zero, which means that the PDF takes an almost symmetric form. Drastic changes occur for $0.65 < D < 0.7$, where the transition between the coherent or quasiordered and fully developed chaotic states occurs. The PDF obtained in this range represents an asymmetric non-Gaussian form because S_N is negative. One should notice that this result is independent of the system size N.

The results obtained in this section are summarized as follows. The spatiotemporal chaotic states are divided into the following three states for each D regions:

(1) $0.55 < D < 0.65$: spatially coherent, quasiordered chaotic state,

(2) $D > 0.7$: fully developed spatiotemporal chaotic state,

(3) $0.65 < D < 0.7$: intermediate or transition state between the states 1 and 2.

In the next section, details of the fluctuation properties of M_t in the transition region 3 will be investigated.

IV. STATISTICAL PROPERTIES OF CHAOTIC RARE FLUCTUATIONS

In the previous section, we investigated the D and N dependences of statistical quantities such as the average a_N and the standard deviation σ_N when M_t fluctuates. In particular, a transition between the quasiordered and the fully developed spatiotemporal chaotic states is observed. In this section, we investigate the spatiotemporal chaotic state observed in this transition range in detail. Numerical simulation of the LCSCM for several D values in this range shows that the universal features of fluctuations being similar to that of BHP [4,9], which will be discussed in the next section, are observed around $D = 0.67$. Therefore, a characteristic value of D in this range is chosen as $D = 0.67$, which is close to the D value giving the largest standard deviation and the smallest skewness coefficient. We analyze the statistical properties of fluctuation of M_t for several system sizes with $D = 0.67$.

First, Fig. 4 shows (a) the time series of M_t and (b) the orbit in the X_t-Y_t plane for $N = 32^2$. Here, the initial condition was chosen as independent random-phase values at each site, which leads to $M_t \simeq 0$. We observe that M_t fluctuates chaotically in the range $0.5 \sim 0.6$. We also observe characteristic rare bursts during which M_t decreases significantly below this range. In this paper, we call these large durations *rare fluctuations*. This result clearly shows that the spatially disordered state comes in the coherent chaotic state. Such rare fluctuations are also observed for other values of D in the transition range, irrespective of N. This is one of the most characteristic aspects of the dynamics in this region. In the X_t-Y_t plane, we see that the orbit moves symmetrically around the origin. This result means that the averaged phase $\overline{\theta_t}$, defined as

$$Z_t = M_t e^{i\overline{\theta_t}}, \tag{15}$$

evolves in time. This behavior is similar to the fact that the total magnetization M_t in the 2DHXY critical spin system fluctuates with changing the averaged orientation rapidly [7].

In order to investigate the statistical properties of the rare fluctuations in detail, we analyze several statistical quantities of M_t. We took 2^{23} data points to calculate the statistical quantities for system sizes $N = 16^2$, 32^2, 48^2, 64^2, and

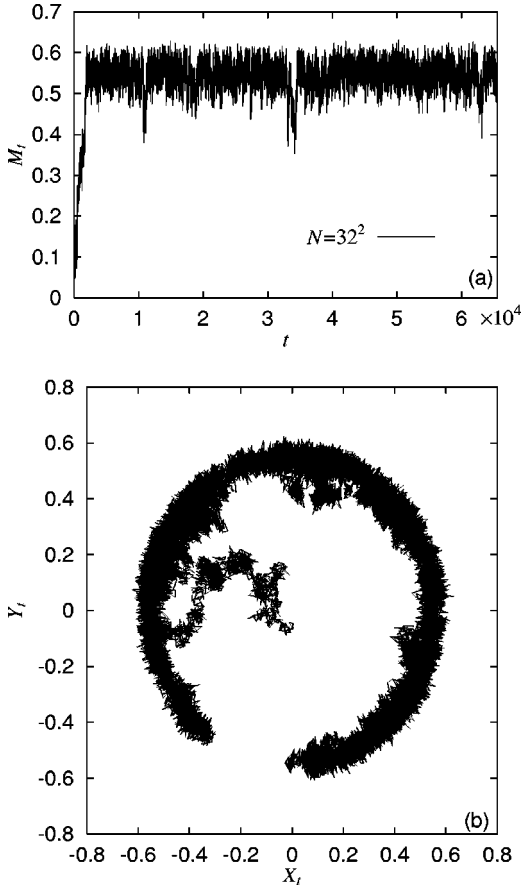

FIG. 4. (a) A short segment of the time series of M_t and (b) the corresponding orbit in X_t-Y_t plane for the LCSCM with $D=0.67$ and $N=32^2$.

80^2, and 2^{24} data points for $N=96^2$ and 128^2. Hereafter, the average operation $\langle \cdots \rangle$ denotes the long-time average over all data points.

Figure 5 shows the PDF of M_t, $P_N(M)=\langle \delta(M-M_t)\rangle$,

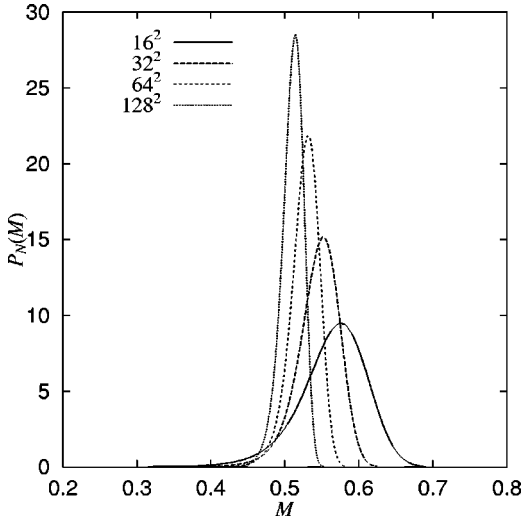

FIG. 5. The probability distribution function $P_N(M)$ calculated from the M_t fluctuations with $D=0.67$ for several system sizes ($N=16^2$, 32^2, 64^2, and 128^2).

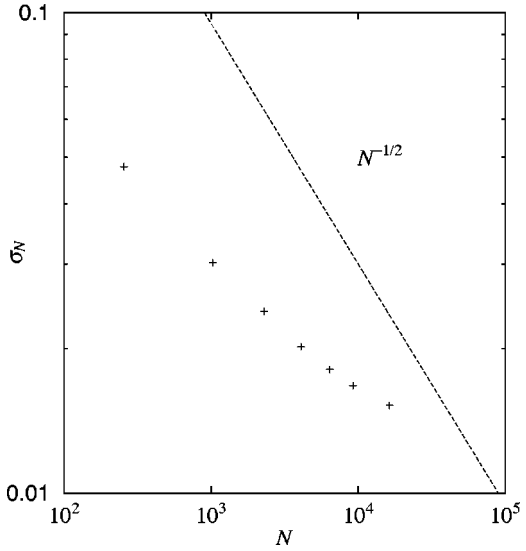

FIG. 6. The dependence on the system size N of the standard deviation σ_N for $D=0.67$. The dotted line denotes $\sigma_N \sim N^{-1/2}$.

calculated for several system sizes. The PDF has a sharp single peak. As N is increased, both the position and the width of the peak decrease. Therefore, a_N is a decreasing function with respect to N, as seen in Fig. 2(a). Figure 6 shows the N dependence of the standard deviation σ_N of the PDF obtained in Fig. 5. It is clearly found that σ_N decreases as N is increased. For a large N, however, it seems that the rate of decay gradually decreases in comparison with that for a small N. It seems that the decaying is not governed by a simple power law. The N dependence of σ_N is interpreted as follows. By using Eq. (15) we can rewrite M_t as

$$M_t=\frac{1}{N}\sum_{\{\mathbf{r}\}=1}^{N}\psi_t(\mathbf{r}), \quad \psi_t(\mathbf{r})=\cos(\theta_t^{(\mathbf{r})}-\overline{\theta_t}). \tag{16}$$

The standard deviation is estimated for $N \gg 1$ by making use of the correlation function of $\psi_t(\mathbf{r})$, $C_N^{\psi}(\mathbf{r})=\langle \psi_t(\mathbf{r})\psi_t(\mathbf{0})\rangle - \langle \psi_t(\mathbf{r})\rangle^2$, as

$$\sigma_N^2 \simeq \frac{2}{N}\sum_{\{\mathbf{r}\}=0}^{N} C_N^{\psi}(\mathbf{r}). \tag{17}$$

If the correlation length of the fluctuations of $\psi_t(\mathbf{r})$ is much shorter than the system size ($\sim\sqrt{N}$), and the N dependence of $C_N^{\psi}(0)$ is negligible in comparison to any power-law function of N, we obtain $\sigma_N \sim N^{-1/2}$ for sufficiently large N. However, Fig. 6 clearly indicates that it decays much slower than $N^{-1/2}$. This result suggests the existence of spatially strong correlations of $\psi_t(\mathbf{r})$, which are closely connected to the existence of a spatial coherent structure.

In order to observe the asymptotic behavior of the PDF, we plot it in a normalized form by using $M \to (M-a_N)/\sigma_N$ and $P_N(M) \to \sigma_N P_N$. The result is shown in Fig. 7. Near the maximum, the PDF takes a parabolic form, but it depends almost linearly on M to the left of the maximum. In short, the PDF shows a strongly asymmetric form, very different from a Gaussian. This asymptotic form is related to the fact that

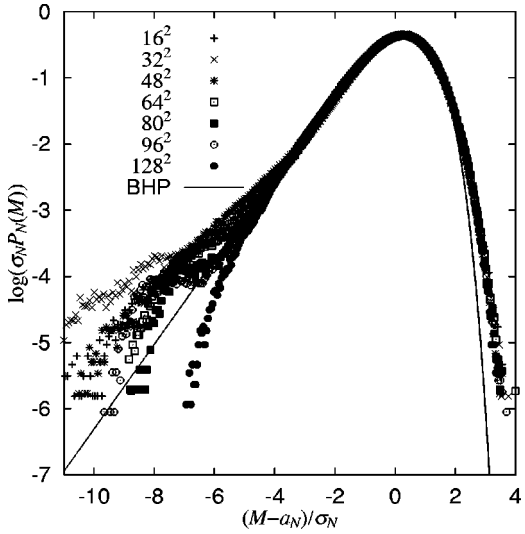

FIG. 7. The normalized probability distribution function of M_t for the LCSCM, shown for several system sizes. The solid curve line represents the BHP fluctuation spectrum Eq. (21). The base of the log is 10.

the skewness coefficient S_N shown in Fig. 3(b) takes negative values. In the range that the deviation from the average value a_N is within $4\sigma_N$, the normalized PDF clearly has a unique form independent of system size N. This means that a scaling law,

$$P_N(M)=\frac{1}{\sigma_N}f\left(\frac{M-a_N}{\sigma_N}\right) \tag{18}$$

is obeyed in a broad range of fluctuation. Here, $f(x)$ is a scaling function that is independent of N and satisfies the normalization conditions

$$\int_{-\infty}^{\infty}f(x)dx=\int_{-\infty}^{\infty}x^2f(x)dx=1, \quad \int_{-\infty}^{\infty}xf(x)dx=0. \tag{19}$$

It is important to notice that the scaling law Eq. (18) leads to relations among moments. If Eq. (18) is satisfied for all ranges of fluctuations, the pth order moments around the average a_N should be represented in terms of σ_N as

$$\langle|M_t-a_N|^p\rangle\simeq k_p\sigma_N^p, \tag{20}$$

with prefactor k_p. Thus, all moments may be determined by σ_N, except for the prefactor k_p. If $\sigma_N\sim N^{-\gamma}$ in a scale range of N, we obtain the relation $\langle|M_t-a_N|^p\rangle\sim N^{-\gamma p}$. The present scaling behaviors are described by just one exponent γ. The numerical result obtained in our model, however, does not show the simple N dependence of σ_N such as $\sigma_N\sim N^{-\gamma}$. The reason that we did not observe the power-law decay of σ_N may be originated from the choosing of the parameter $D=0.67$, which seems to be slightly smaller than just a transition point D_c. If we choose $D=D_c$, the spatial correlation of fluctuations is strongest in this point, and may observe the power-law decay.

Moreover, we refer to the N dependence of the normalized PDF in the extreme left of Fig. 7. We consider that this N dependence is not the statistical error because the right extreme is perfectly in agreement with the scaling law. We doubt that the statistical property of the extremely rare fluctuations are sensitively depending on the parameter D below a transition point D_c and the system size N. If we take just a transition parameter, the unique behaviors of a whole range of fluctuations will be observed. This is one of the possibilities of the observed N dependence, and an unsolved problem in the present paper.

The statistical nature of the rare fluctuations obtained in this section suggests that a unique, non-Gaussian PDF exists, irrespective of N in a broad range of fluctuations. This property is quite similar to that of the universal PDF suggested for turbulence and critical phenomena by BHP [4]. The relation between our results and that of BHP is discussed in the next section.

V. UNIVERSAL DISTRIBUTION FUNCTION FOR RARE FLUCTUATIONS

In the previous section, we showed that the fluctuations of M_t are characterized by rare, large bursts that are called rare fluctuations. Furthermore, it was shown that the normalized PDF obtained from the rare fluctuations is a non-Gaussian, unique function that is independent of the system size N in a broad range. It is quite tempting to attempt to obtain the analytical form of the PDF. The fluctuations of M_t are deterministically produced by the fundamental dynamical LCSCM system. The numerical results discussed in Sec. IV suggest that the PDF obtained for the LCSCM is expected to be similar to the universal PDF proposed by BHP [4]. However, it is rather difficult to theoretically determine the form of the PDF for the LCSCM. Instead, we will therefore use analytical results for the 2DHXY model, for which some statistical quantities related to the magnetic scalar fluctuations can be exactly derived [7–9,17]. In particular, a unique form for the PDF form for the magnetic fluctuations in the low-temperature region is investigated in detail. The origin of the non-Gaussian nature of the PDF and its independence of N are discussed in [8] by evaluating the functional form of the PDF from relations among moments. Moreover, the asymptotic form of the universal PDF, which we call the ''BHP fluctuation spectrum,''

$$f(x)=K\exp\left[\frac{\pi}{2}\{b(x-s)-e^{b(x-s)}\}\right] \tag{21}$$

is suggested in [9], where it is shown that Eq. (21) is in good agreement with numerical results. The parameters in Eq. (21) ($K=2.14$, $b=0.938$, and $s=0.374$) are constants evaluated by Eq. (19). In addition, the details of the fitting of Eq. (21) and other functional forms for the universal PDF by BHP are discussed in [17]. Furthermore, it is shown in [9] that PDF's of global measure fluctuations defined in several correlated systems, such as self-organized criticality or percolation systems, are in good agreement with the BHP function (21).

The chaotic model treated in this paper seems to be in a critical state for $D=0.67$ because it is near the transition point between the quasiordered and fully developed chaotic

states. Moreover, strong spatial correlations appear in this range, evidenced by the fact that the standard deviation σ_N decreases more slowly than $N^{-1/2}$ as shown in Fig. 6. We therefore conclude that the present LCSCM model possesses strong spatial correlations. Thus, we suspect that our PDF may belong to the same universality class as the BHP fluctuation spectrum. In order to test this possibility, our results are compared with the BHP form in Fig. 7. The result represents that the PDF of the LCSCM seems to be in good agreement with the BHP form over the wide range of fluctuations, but slightly deviates from it in the tail regions.

Here, we consider the origin of the deviations in the tail regions of PDF. In general, it is uncertain to apply BHP form evaluated in theoretical studies of the 2DHXY model to other systems. The LCSCM has the same spatial dimension and the same symmetry as the 2DHXY model. Nevertheless, it is quite natural that rare fluctuation induced by thermal noise in the 2DHXY model may be different from those induced by chaotic coherent noise produced by the strong nonlinearity of the LCSCM. Moreover, it is reported in [18] that the 2DXY model for temperatures close to the Kosterlitz-Thouless transition shows a significant deviation from the BHP form, so that the harmonic (spin-wave) approximation is needed to obtain the BHP fluctuation spectrum in the 2DXY model. This fact provides a hint as to the origin of the disagreement of our results with the BHP form. In order to discuss this problem, we propose a model that amounts to a ''harmonic approximation'' to the LCSCM, and we compare its order-parameter fluctuations to those of the LCSCM.

If the phase differences among nearest neighbors are sufficiently small, i.e., a closely synchronized state, we can approximate the interaction term as $\sin(\theta_t^{(x',y')}-\theta_t^{(x,y)}) \simeq \theta_t^{(x',y')}-\theta_t^{(x,y)}$. Moreover, we expect that the fluctuations induced by chaos plays a role to disturb the phases. This is taken into account in the linearized model by introducing a stochastic noise. Consequently, the phenomenological stochastic phase map model we propose takes the form,

$$\theta_{t+1}^{(x,y)} = \theta_t^{(x,y)} + D\sum_{n.n.} (\theta_t^{(x',y')} - \theta_t^{(x,y)}) + f\Gamma_t^{(x,y)}. \quad (22)$$

The parameter f controls the intensity of the external noise term, where $\Gamma_t^{(x,y)}$ is a uniform random variable on $[-1,1]$, statistically independent at each site and time step. Here we note a difference in the physical significance of D between the LCSCM and Eq. (22). The parameter D in the LCSCM controls the state of chaotic motion for $D>1/4$, where the nonlinearity plays an important role for the dynamics. On the other hand, the linearized LCSCM is meaningful only for $0<D<1/4$ because its solutions for $D>1/4$ are unstable, as seen from the stability condition of Eq. (22) with $f=0$. Therefore, D should be limited to $0<D<1/4$ in Eq. (22). In this case, D is regarded as a phase diffusion coefficient, which controls the degree of synchronization among phases, because the continuous limit of Eq. (22) without external noise is equivalent to the phase diffusion equation. The diffusion term promotes relaxation towards a state of fully synchronized phases. Therefore, the value of M_t approaches unity if the external noise term is neglected in Eq. (22). This is the reason for the necessity of the external forcing. Hereafter, Eq. (22) will be called the random phase diffusion map (RPDM).

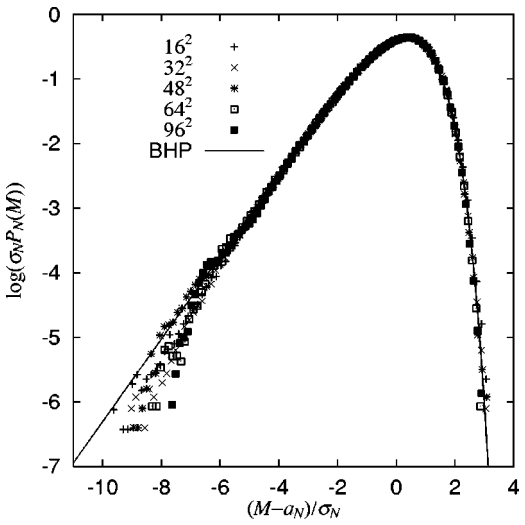

FIG. 8. The normalized probability distribution function of M_t in the RPDM for several system sizes. The solid curve represents the BHP fluctuation spectrum Eq. (21). The base of the log is 10.

We have solved the RPDM numerically and observed the fluctuations of the order-parameter M_t. The parameters in the RPDM are D, f, and N. The parameter f measures the intensity of the agitation. We study the properties of M_t in the small f regime. By performing the numerical simulation of the RPDM for several parameter values, we find that there exists a unique PDF independent of D and N as long as $f \ll 1$ is satisfied. The results for $D=0.1$ and $f=0.15$ are shown in Fig. 8 for $N=16^2$, 32^2, 48^2, 64^2, and 96^2, where the PDF's are normalized as those in Fig. 7. The characteristics of the PDF in Fig. 8 are (i) the PDF takes an asymmetric non-Gaussian form that is similar to that obtained for the LCSCM, (ii) the normalized PDF seems to be independent of the system size N in the whole range of fluctuation, and (iii) the normalized PDF is in good agreement with the BHP fluctuation spectrum.

One should notice that the RPDM is equivalent to the Langevin equation for the 2DHXY model if we take the continuous time limit. Therefore, the PDF of M_t obtained by the RPDM in this paper is same as that obtained by BHP in [4,9]. This is the reason that the PDF for the RPDM is in good agreement with the BHP form. On the other hand, it is interesting to note that the functional form obtained in the LCSCM is quite similar to that in the BHP form (21). This is because the rare fluctuations in the LCSCM are caused by deterministic chaos. Why are both PDFs so similar?

We anticipate that the main mechanism producing the rare fluctuations is the competition between processes that synchronize and disturb the individual phases. In the RPDM, these mechanisms are the ''diffusion term'' and the ''noise term,'' respectively. On the other hand, these mechanisms do not exist independently in the LCSCM. For the intermediate coupling range in the LCSCM, however, we expect that the coherent chaotic dynamics plays a role in producing both

mechanisms because the dynamics is represented by the coexistence of the quasiordered, coherent state and the fully developed spatiotemporal chaotic one. It is possible that the fully developed chaotic dynamics play the role of ''noise term'' in the RPDM. Conversely, the quasiordered dynamics seem to promote the synchronization among phases. As a result, the intermediate chaotic state contains two mechanisms implicitly. One should, however, notice that the quasiordered state is also weakly chaotic, so that the dynamics are also affected by the nonlinearity. Thus, the role of the intermediate state is different from that of a simple ''diffusion term,'' which is linear in $\theta_t^{(x,y)}$. Under this consideration, we conclude that the qualitative features of the rare fluctuations in the LCSCM are different from those of the RPDM, since the deviation from the BHP form for the LCSCM originates from the spatially quasiordered chaotic state of the system.

VI. POWER SPECTRUM FOR RARE FLUCTUATION DYNAMICS

As shown in the previous sections, the form of the PDF for the LCSCM is quite close to the universal PDF proposed by BHP. However, the universal nature of fluctuations proposed by BHP [4,9] is based on the resemblance between the PDF's of global measures in different systems, i.e., static properties. The dynamical statistics of rare fluctuations have not been discussed in those studies. It is an important problem to elucidate the statistical properties of temporal correlations of rare fluctuations in correlated physical systems that share the BHP fluctuation spectrum. In this section, we investigate the N dependence of temporal correlations.

It is useful to investigate the spectral density of order-parameter fluctuations $\Delta M_t = M_t - \langle M_t \rangle$, defined by

$$I_N(\omega_k) = \left\langle \left| \sum_{t=0}^{T-1} \Delta M_t e^{i\omega_k t} \right|^2 \right\rangle \tag{23}$$

for several system sizes. Here, $t=0,1,2,\ldots,T-1$ and $\omega_{k=\omega} = 2\pi k/T (k=0,1,2,\ldots,T-1)$. The $I_N(\omega_k)$ are normalized so as to satisfy $C_N(0) = \sigma_N^2 = \Sigma_{k=0}^{T-1} I_N(\omega_k)/T$, where $C_N(t)$ is the autocorrelation function of M_t, i.e., $C_N(t) = \langle \Delta M_t \Delta M_0 \rangle$. Figure 9 shows the numerical results for the power spectrum of M_t in the LCSCM for $T=32\,768$ ($N = 16^2$, 32^2, 48^2, 64^2, and 80^2) and $T=65536$ ($N=96^2$ and 128^2). One clearly observes that $I_N(\omega)$ is almost constant in the low-frequency region, but asymptotically takes a power-law $\omega^{-(1+\alpha)}$ with a positive α in the moderately high-frequency region. This power law is characterized by an excess exponent α, which is numerically estimated as $\alpha = 0.6 \sim 0.7$. Moreover, observe that α for large N is independent of N. For the reference, we plot $\omega^{-(1+\alpha)}$ with $\alpha = 0.7$ in Fig. 9. On the other hand, one may notice that a small bump exists in the right extreme tail of $I_N(\omega)$. The peak position of bump for each N is about half of the Nyquist frequency and independent of N. This result may denote the short-time coherent dynamics of the system originated from the characteristics of chaotic behavior of the individual oscillator. The asymptotic power spectra for large N are so similar to the Lorentzian that is obtained by Fourier transformation of an exponentially decaying autocorrelation function, though the scaling exponent clearly deviates from the case of a Lorentzian tail ($\alpha = 1$). For $0 < \alpha < 1$, however, the autocorrelation function may be a stretched exponentially decaying function [19,20] as

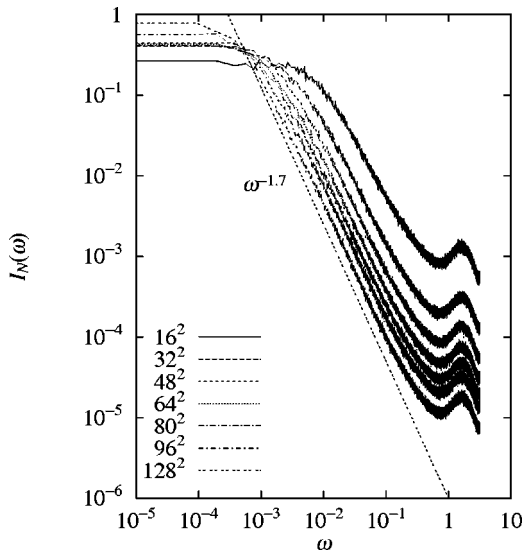

FIG. 9. The power spectra $I_N(\omega)$, calculated from the time series of M_t in the LCSCM for several system sizes. The reference line has a slope of -1.7.

$$C_N(t) = C_N(0) \exp\left(-\left| \frac{t}{\tau_N} \right|^{\alpha} \right), \tag{24}$$

where τ_N represents the characteristic correlation time of M_t, which depends on the system size N. In order to check the form of Eq. (24), we evaluate $C_N(t)$ from the numerical results of $I_N(\omega)$ in Fig. 9 by the Wiener-Khinchin theorem. The plot is shown in Fig. 10 for $C_N(t)/C_N(0)$ vs t^{α} with α

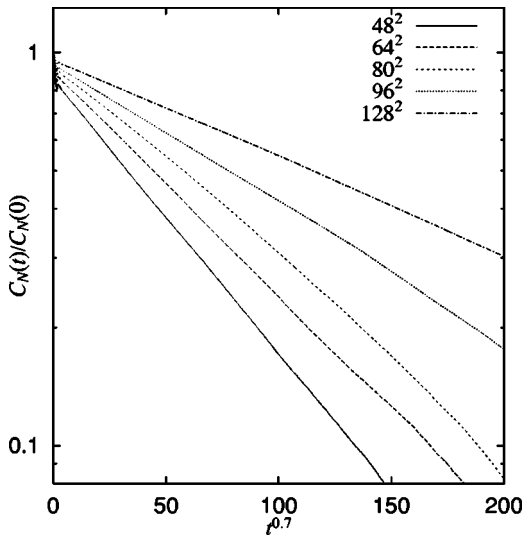

FIG. 10. The autocorrelation function of the LCSCM evaluated by $I_N(\omega)$ in Fig. 9 for several system sizes. One should notice that the horizontal axis is made by $t^{0.7}$.

$=0.7$ for $N=48^2$, 64^2, 80^2, 96^2, and 128^2 via a semi-log plot. The results clearly indicate that $C_N(t)$ is well represented by the stretched exponential form except the small t region. This deviation from Eq. (24) in small t region is due to the bump of $I_N(\omega)$ in the high-frequency region. As N increased, $C_N(t)$ decreases more slowly in time. This result implies that the characteristic times τ_N is the increasing function of N. Thus, the autocorrelation function is asymptotically given by the stretched exponential function. On the other hand, this result is also verified as follows. If the asymptotic form (24) is held in the whole range of time steps, the power spectrum evaluated by using Wiener-Khinchin theorem has the scaling form

$$I_N(\omega)=I_N(0)g\left(\frac{\omega}{\omega_N}\right), \tag{25}$$

with the characteristic frequency $\omega_N=2\pi/\tau_N$, where $g(x)$ is a scaling function independent of N. If T is sufficiently larger than the discrete time interval, we can take the continuous time limit, and the summation is replaced by an integral. In this case, $g(x)$ is represented by

$$g(x)=\frac{\int_0^\infty e^{-z^\alpha}\cos(2\pi zx)dz}{\int_0^\infty e^{-z^\alpha}dz}. \tag{26}$$

In order to investigate the above-mentioned features of the temporal correlations, we check the validity of the scaling law (25). For this purpose, we must estimate the characteristic frequency (time) $\omega_N(\tau_N)$ in a concrete manner. Supposing that the autocorrelation function is represented by Eq. (24) in a broad time range, we may estimate the explicit form of τ_N by substituting $C_N(t)=C_N(0)\exp(-|t/\tau_N|^\alpha)$ into $I_N(\omega)=2\int_0^\infty C_N(t)\cos(\omega t)dt$ as

$$\tau_N=\frac{\alpha I_N(0)}{2C_N(0)\Gamma(1/\alpha)}, \tag{27}$$

where $\Gamma(z)$ is the Gamma function. Consequently, τ_N is evaluated by using numerical results for $I_N(0)$, $C_N(0)$, and the scaling exponent α, α being estimated from the asymptotic form of the power spectrum.

Figure 11 shows the scaling plot for several system sizes with $\omega_N=2\pi/\tau_N$ evaluated by Eq. (27), where α is taken as $\alpha=0.7$. The scaling law works very well in the whole frequency range except the highest-frequency tail. This result also supports that the autocorrelation function is asymptotically represented by a stretched exponential function. Moreover, we can obtain the asymptotic form of the scaling function $g(x)$ (26) with $x\gg1$ as [20],

$$g(x)\sim A(\alpha)x^{-(1+\alpha)},\quad A(\alpha)=\frac{\alpha\Gamma(\alpha+1)\sin(\pi\alpha/2)}{\Gamma(1/\alpha)(2\pi)^{1+\alpha}}$$

$$(x\gg1). \tag{28}$$

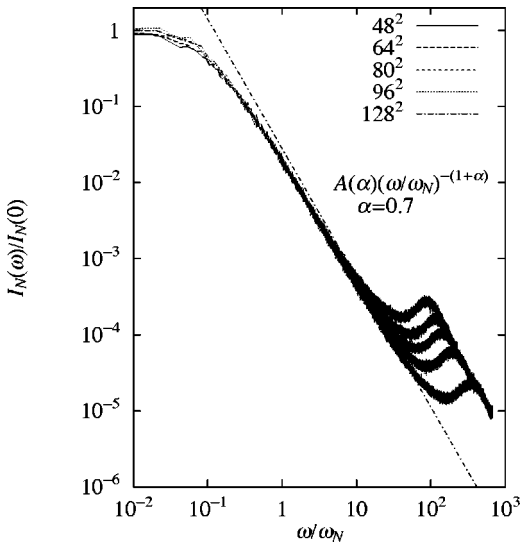

FIG. 11. Scaling plot of $I_N(\omega)$ from Fig. 9. The reference line shows the asymptotic form of the scaling function $g(\omega/\omega_N)$ [Eq. (28)] with $\omega/\omega_N\gg1$ evaluated by assuming the stretched-exponential form of the autocorrelation function, $C_N(t)=C_N(0)\exp(-|t/\tau_N|^{0.7})$. Here, $\omega_N=1.82$, 1.39, 1.15, 0.83, and 0.47 $(\times10^{-2})$ for $N=48^2$, 64^2, 80^2, 96^2, and 128^2.

The asymptotic form (28) with $\alpha=0.7$ are drawn in Fig. 11. The result is in agreement with the numerical ones for $\omega\geqslant\omega_N$, but seems to slightly deviate from the numerical result. This is originated from the overestimation of ω_N because the bump structure of $I_N(\omega)$ in the highest-frequency region (or oscillatory structure of $C_N(t)$ in $t^\alpha\ll1$) affects the correct values of ω_N when we evaluate them by supposing the pure stretched exponential form of $C_N(t)$.

We have also calculated power spectra for the RPDM. The asymptotic form of the power spectra is found to be similar to the case of the LCSCM, viz. $I_N(\omega)\sim$ Const. in the low-frequency region and $I_N(\omega)\sim\omega^{-(1+\alpha)}(\alpha\simeq0.8)$ in the high-frequency one. The scaling exponent α for the RPDM seems to be slightly larger than that for the LCSCM. We evaluate the autocorrelation function $C_N(t)$ in RPDM by using the results of $I_N(\omega)$, as done in LCSCM. The results are shown in Fig. 12 via a semi-log plot of $C_N(t)/C_N(0)$ vs $t^{0.8}$. This result clearly shows that the autocorrelation functions for each N are well expressed by the stretched exponentially decaying function (24) with $\alpha=0.8$ in the whole range of time.

Moreover, we investigate the scaling law of the power spectra as done in the case of LCSCM, but putting $\alpha=0.8$. As shown in Fig. 13, the scaling law works very well in the whole frequency region, i.e., $I_N(\omega)/I_N(0)=g(\omega/\omega_N)$. The asymptotic form of $g(x)$ with $x\gg1$ is also drown in Fig. 13 with $\alpha=0.8$, which is in good agreement with the numerical results. Therefore, we conclude that the autocorrelation function of M_t in the RPDM is quite well expressed by a stretched exponential function, as in the LCSCM case. This is an interesting result because the dynamical properties of the nonequilibrium chaotic system such as the LCSCM is quite similar to that of the equilibrium RPDM model. The similarity of static and dynamic properties between the

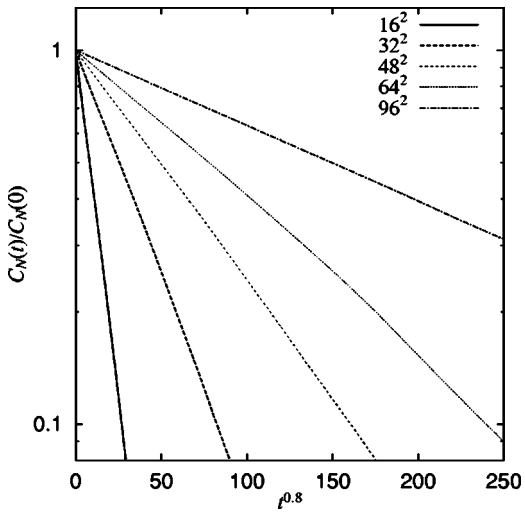

FIG. 12. The autocorrelation function of the RPDM evaluated by $I_N(\omega)$ for several system sizes. One should notice that the horizontal axis is made by $t^{0.8}$.

LCSCM and the RPDM suggests the possibility that there exists a universal dynamical equation for describing the order-parameter fluctuation. If so, such an equation will be, of course, established in the coarse-grained levels of fluctuation, where the origins of fluctuation is clearly different each other in the microscopic level. It is an important and interesting problem to construct the governing equation of motion for M_t fluctuation.

Finally, we comment on the N dependence of the characteristic frequency ω_N. We have referred to the fact that the continuous limit of the RPDM leads to the diffusion equation without an external noise term, $\dot{\theta}(x,y,t)=D_{diff}\nabla^2\theta(x,y,t)$.

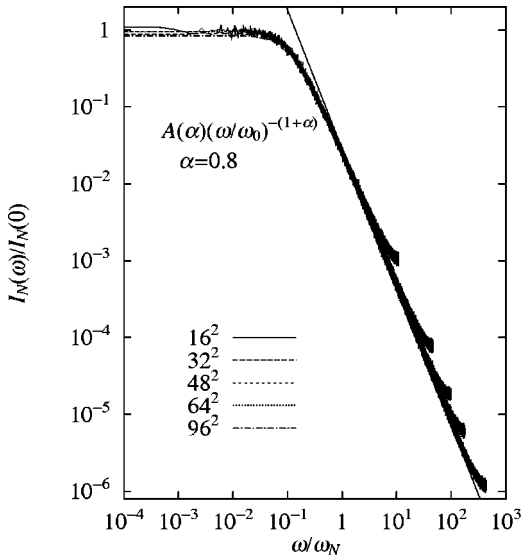

FIG. 13. Scaling plot of $I_N(\omega)$, calculated from M_t in the RPDM. The reference line shows the asymptotic form of the scaling function $g(\omega/\omega_N)$, Eq. (28) with $\omega/\omega_N \gg 1$ evaluated by assuming the stretched-exponential form of the autocorrelation function, $C_N(t)=C_N(0)\exp(-|t/\tau_N|^{0.8})$. Here, $\omega_N=28.64$, 6.75, 3.21,1.75, and 0.71 $(\times 10^{-2})$ for $N=16^2$, 32^2, 48^2, 64^2, and 96^2.

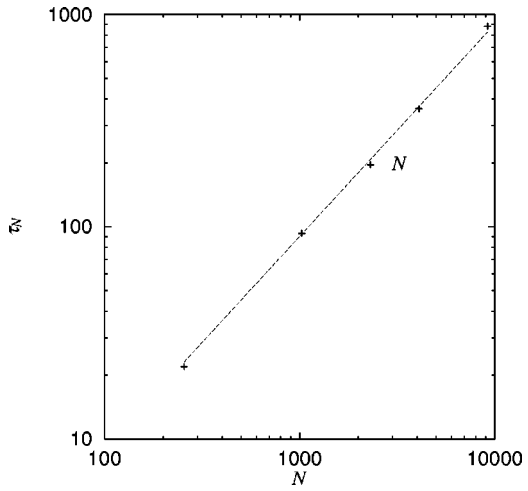

FIG. 14. The N dependence of the characteristic time τ_N in the RPDM evaluated by Eq. (27). The dotted line represents $\tau_N \sim N$, which is estimated by the dimensional arguments. For details, see the text.

By dimensional analysis of the diffusion equation, we can estimate the N dependences of ω_N as follows. The scaling relation between the characteristic length scale L and the time scale T is represented by the diffusion equation as $T^{-1}\sim D_{diff}L^{-2}$. In the 2D system, the system size N is evaluated by $N\sim L^2$, which leads to the evaluation $\omega_N \sim T^{-1}\sim D_{diff}N^{-1}$, if ω_N is regarded as the inverse of the characteristic time. Figure 14 shows the N dependence of characteristic time τ_N evaluated by Eq. (27) in RPDM. We can recognize that the prediction by dimensional analysis of phase diffusion equation works very well, i.e., $\tau_N \sim N$.

VII. SUMMARY

In this paper, we have investigated the statistical properties of rare fluctuations of the order-parameter M_t in the LCSCM. Universal statistical properties with respect to variation of the system size N were explored by numerical simulations. As a result, we have found that the steady-state distribution function in a characteristic spatiotemporal chaotic state is a non-Gaussian function, and that the functional form of the normalized distribution function is independent of the system size N. The form of the PDF obtained for the LCSCM was discussed in connection with the BHP fluctuation spectrum and, on the whole, was in good agreement with it. The results obtained in this paper may suggest that there exist universal statistical features common to turbulence, critical phenomena, and dissipative systems.

Furthermore, we have investigated the dynamical properties of rare fluctuations, which have not previously been discussed for universal rare fluctuations. It was found that the power spectrum of the order-parameter fluctuations has the power-law form $\omega^{-(1+\alpha)}$ with $\alpha=0.6\sim 0.7$ for the LCSCM and $\alpha=0.7\sim 0.8$ for the RPDM, in the high-frequency region below the Nyquist frequency. Moreover, we have discussed the existence of a scaling law for the power spectrum, independent of the system size N. These results may imply that the autocorrelation function for rare fluctuations is expressed

by a stretched-exponential function. The temporal correlations with stretched exponential decay found in this paper imply that the correlations decay more slowly than conventional fluctuations that obey exponential decay. However, the stretched-exponential decay is faster than the power-law that is obtained as $\exp(-|t/\tau|^{\alpha})$ in the $\alpha \to 0$ limit. When the autocorrelation function decays as a power law, the statistical analysis based on the large deviation theory for strongly correlated time series is applied to characterize the intermittent time series [3]. It is an interesting problem how such fluctuations can be characterized by large deviation statistics.

The rare fluctuations observed in this paper with $D=0.67$ are also observed for the other parameter values of D in the transition region $0.65<D<0.7$, as discussed in Sec. III. From the statistical viewpoint of the critical phenomena, the statistical and dynamical properties of the rare fluctuations in just a critical value D_c is interesting, though the value $D=0.67$ treated in the present paper seems to be near D_c. The important problem is to determine a value D_c in the infinite system size by using the finite-size scaling. If we obtain the critical value D_c, it is also interesting to investigate the several aspects of rare fluctuations with $D=D_c$. The strong spatial correlation of fluctuations and finite-size scaling will be reported in a future paper.

It is well known that the vortex formation in the 2DXY system plays a crucial role in its critical dynamics [2]. To discuss the universal probability density (21) and the stretched exponential decay of the time correlation function (24) in connection with the vortex dynamics is particularly interesting. Studies in this direction in a future are highly desired.

Finally, we comment on how the spatial dimensionality and the boundary conditions influence the form of the PDF for rare fluctuations. First, we cannot necessarily observe rare fluctuations for all values of D in the one-dimensional (1D) case of the LCSCM. The dynamics of M_t in the 1D-LCSCM shows chaotic behavior for $D>0.5$, but it seems that the transition between weak and fully developed chaotic states occurs at a specific value of D. This implies that no intermediate region is observed in the 1D case. Consequently, the present chaotic map model indicates large differences in the spatiotemporal dynamics between 1D and 2D systems. It is also important to study 3D-LCSCM systems. To clarify the difference of its dynamical behavior from 1D and 2D systems is interesting. However, the study on 3D systems is beyond the scope of the present paper. Second, we have clarified that the BHP fluctuation spectrum obtained for the RPDM is not observed if we do not require periodic boundary conditions [15]. However, the obtained PDF is qualitatively similar to the BHP but is quantitatively different from it. This result clearly indicates that finite-size effects affect the statistical properties of global fluctuations. The effects of the boundary conditions will be reported in a future paper.

ACKNOWLEDGMENTS

One of the authors (T.W.) thanks Professor P. A. Rikvold for the critical reading of the manuscript, useful comments, and discussions.

[1] U. Frisch, *Turbulence* (Cambridge University Press, Cambridge, 1995).
[2] N. Goldenfeld, *Lectures on Phase Transitions and the Renormalization Group* (Addison-Wesley, Reading, MA, 1992); L. P. Kadanoff, *Statistical Physics - Statics, Dynamics and Renormalization* (World-Scientific, Singapore, 2000).
[3] H. Fujisaka and M. Inoue, Prog. Theor. Phys. **77**, 1334 (1987); T. Watanabe, Y. Nakayama, and H. Fujisaka, Phys. Rev. E **61**, R1024 (2000); H. Fujisaka, H. Suetani, and T. Watanabe, Prog. Theor. Phys. Suppl. **139**, 70 (2000).
[4] S. T. Bramwell, P. C. W. Holdsworth, and J.-F. Pinton, Nature (London) **396**, 552 (1998).
[5] R. Labbe, J.-F. Pinton, and S. Fauve, J. Phys. II **6**, 1099 (1996).
[6] J.-F. Pinton, P. C. W. Holdsworth, and R. Labbé, Phys. Rev. E **60**, R2452 (1999).
[7] P. Archambault, S. T. Bramwell, and P. C. W. Holdsworth, J. Phys. A **30**, 8363 (1997).
[8] P. Archambault, S. T. Bramwell, J-Y Fortin, P. C. W. Holdsworth, S. Peysson, and J-F Pinton, J. Appl. Phys. **83**, 7234 (1998).
[9] S. T. Bramwell, K. Christensen, J.-Y. Fortin, P. C. W. Holdsworth, H. J. Jensen, S. Lise, J. M. López, M. Nicodemi, J.-F. Pinton, and M. Sellitto, Phys. Rev. Lett. **84**, 3744 (2000).
[10] H. Mori and Y. Kuramoto, *Dissipative Structures and Chaos* (Springer, Berlin, 1998).
[11] T. Bohr, M. Jensen, G. Paladin, and A. Vulpiani, *Dynamical Systems Approach to Turbulence* (Cambridge University Press, Cambridge, 1998).
[12] S. Uchiyama and H. Fujisaka, Phys. Rev. E **56**, 99 (1997).
[13] A. J. Noest, Europhys. Lett. **6**, 469 (1988); Phys. Rev. A **38**, 2196 (1988).
[14] S. Uchiyama and H. Fujisaka, J. Phys. A **32**, 4623 (1999); S. Uchiyama, Ph.D. thesis, Department of Physics, Kyushu University, Fukuoka, Japan (2000).
[15] Y. Tsubo, Master thesis, Graduate School of Informatics, Kyoto University, Japan (2000), in Japanese.
[16] K. Kaneko, Physica D **54**, 5 (1991).
[17] S. T. Bramwell, J.-Y. Fortin, P. C. W. Holdsworth, S. Peysson, J.-F. Pinton, B. Portelli, and M. Sellitto, Phys. Rev. E **63**, 041106 (2001).
[18] V. Aji and N. Goldenfeld, Phys. Rev. Lett. **86**, 1007 (2001).
[19] W. Feller, *An Introduction to Probability Theory and Its Applications*, 2nd ed. (Wiley, New York, 1971), Vol. 2.
[20] E. W. Montroll and J. T. Bendler, J. Stat. Phys. **34**, 129 (1984).